How DNA coiling enhances target localization by proteins

B. van den Broek*†, M. A. Lomholt‡, S.-M. J. Kalisch*§, R. Metzler¶, and G. J. L. Wuite*‖

*Department of Physics and Astronomy, Faculty of Sciences, Vrije Universiteit, De Boelelaan 1081, 1081 HV Amsterdam, The Netherlands; ‡MEMPHYS Center for Biomembrane Physics, Department of Physics and Chemistry, University of Southern Denmark, Campusvej 55, 5230 Odense M, Denmark; and ¶Physik Department, Technical University of Munich, James Franck Strasse, 85747 Garching, Germany

Edited by Peter H. von Hippel, University of Oregon, Eugene, OR, and approved July 24, 2008 (received for review May 1, 2008)

Many genetic processes depend on proteins interacting with specific sequences on DNA. Despite the large excess of nonspecific DNA in the cell, proteins can locate their targets rapidly. After initial nonspecific binding, they are believed to find the target site by 1D diffusion (''sliding'') interspersed by 3D dissociation/reassociation, a process usually referred to as facilitated diffusion. The 3D events combine short intrasegmental ''hops'' along the DNA contour, intersegmental ''jumps'' between nearby DNA segments, and longer volume ''excursions.'' The impact of DNA conformation on the search pathway is, however, still unknown. Here, we show direct evidence that DNA coiling influences the specific association rate of EcoRV restriction enzymes. Using optical tweezers together with a fast buffer exchange system, we obtained association times of EcoRV on single DNA molecules as a function of DNA extension, separating intersegmental jumping from other search pathways. Depending on salt concentration, targeting rates almost double when the DNA conformation is changed from fully extended to a coiled configuration. Quantitative analysis by an extended facilitated diffusion model reveals that only a fraction of enzymes are ready to bind to DNA. Generalizing our results to the crowded environment of the cell we predict a major impact of intersegmental jumps on target localization speed on DNA.

DNA configuration | DNA–protein interaction | facilitated diffusion | intersegmental jumping | single-molecule

An essential feature in biological processes on DNA is the ability of proteins to quickly locate specific DNA sequences in a vast surplus of nonspecific DNA (1, 2). A protein's search for the target site is thought to be accelerated by facilitated diffusion along nonspecific DNA (3–6). Recent work has yielded considerable insight in the possible search strategies of site-specific proteins (7–15). Assisted by DNA looping some proteins can, for instance, intermittently bind to two DNA segments simultaneously. This way they can directly move from one to another chemically remote segment (16). This intersegmental transfer accelerates target finding on DNA because it assumes a constantly changing random configuration (11). Here, we demonstrate and quantify a similar mechanism, intersegmental jumping, for proteins with only one DNA-binding site.

Little experimental work on facilitated diffusion is available. To date, most studies have been investigating DNA cleavage by restriction enzymes in bulk assays, measuring association times as a function of DNA length, or monitoring processivity on DNA constructs with two sites (7, 17–21). Although in these biochemical assays valuable information can be obtained, association rates of proteins to specific sites are difficult to measure, and the underlying kinetics of the target search mechanism are often obscured. Furthermore, it remains experimentally challenging to distinguish 1D and 3D search pathways. In previous single-molecule assays only pure 1D protein search has been addressed (21–24). Here, we present single-molecule measurements of DNA cleavage by EcoRV on individual plasmid-size molecules (6,538 bp; one EcoRV site) having different degrees of conformational freedom. By tuning the DNA extension, the conformation of the DNA can be changed from a relaxed random configuration to an extended polymer. This procedure enables us to selectively ''switch off'' 3D intersegmental jumping, while leaving sliding, intrasegmental hopping, and long volume excursions intact. By acquiring specific association rates of EcoRV for these DNA conformations at different salt conditions, we can thus determine the relative impact of 3D intersegmental jumps (illustrated in Fig. 1 *A* and *B*) on the search process.

Results and Discussion

Experimental Approach. To determine the bimolecular association rate k_{on} to a recognition site on linear DNA, for different polymer conformations, individual DNA molecules were tethered between two optically trapped beads in a multichannel flow chamber as described (25, 26). The degree of DNA coiling was set by changing the distance between the two beads (Fig. 1*C*). After the buffer flow was stopped DNA constructs were quickly ($\approx$0.5 s) transported into enzyme solution. The DNA molecule was briefly ($<$20 ms) stretched to a force of 5–10 pN every second, to check whether it was cut [supporting information (SI) Movie S1]. The transient stretching resulted in spikes in the force trace that disappeared when the DNA had been cleaved in the preceding second (Fig. 2). The cleavage time was defined as the time between moving the construct into the enzyme solution and scission of both DNA strands.

As we are interested in the influence of DNA configuration on the association rate, the complete cleavage reaction (comprising association, induced fit, DNA hydrolysis, and product release) should be limited by diffusion of the protein to the specific site. We have previously demonstrated that the induced-fit process at low DNA tension is very fast and that product release from the plasmid, in bulk experiments normally the slowest step (27, 28), is not rate-limiting in our optical tweezers experiments (25). This result leaves the actual strand cleavage reaction, the hydrolysis of two phosphodiester bonds in the DNA backbone, as a possible rate-limiting step. This latter rate was determined by measuring cleavage times of pCco5 DNA molecules in a stretched configuration at saturating enzyme conditions (500 nM) (Fig. 3). The rate of strand cleavage was found to be 0.60 s^{-1}. Consequently, the average time needed for the cleavage of both strands is 2.5 s. To satisfy the diffusion-limited requirement mentioned above, and to avoid fluc-

Author contributions: B.v.d.B. and G.J.L.W. designed research; B.v.d.B. and S.-M.J.K. performed research; B.v.d.B., M.A.L., S.-M.J.K., R.M., and G.J.L.W. analyzed data; and B.v.d.B., M.A.L., S.-M.J.K., R.M., and G.J.L.W. wrote the paper.

The authors declare no conflict of interest.

This article is a PNAS Direct Submission.

†Present address: Physics of Life Processes, Leiden Institute of Physics, Leiden University, Niels Bohrweg 2, 2333 CA Leiden, The Netherlands.

§Present address: FOM Institute for Atomic and Molecular Physics, Kruislaan 407, 1098 SJ Amsterdam, The Netherlands.

‖To whom correspondence should be addressed. E-mail: gwuite@few.vu.nl.

This article contains supporting information online at www.pnas.org/cgi/content/full/0804248105/DCSupplemental.

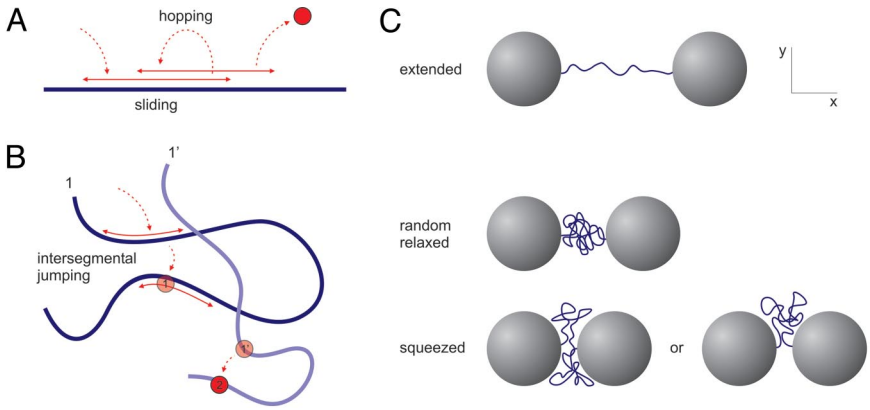

Fig. 1. Protein search pathways and experimental approach. (*A*) Facilitated diffusion model with sliding and hopping resulting in probing of already visited sites (oversampling) on straight DNA. (*B*) On coiled DNA the enzyme can be captured by a segment it has not yet visited, leading to an intersegmental jump and reduction of oversampling. Because of random polymer fluctuations a protein performing an intersegmental jump at instant 1 will, upon unbinding at instant 1′ have moved far away from the original segment, accelerating the search process. (*C*) Experimental approach. Single DNA molecules are held between two beads in optical tweezers. EcoRV cleavage rates are measured at different DNA extensions. The conformational freedom of the DNA at these extensions can be divided into three regimes: (entropically) stretched DNA (*Top*), globular DNA (relaxed coil) (*Middle*), and a DNA coil that is squeezed between the beads. (*Bottom*)

tuations in enzyme concentration caused by adsorption onto the walls and tubing of the flow chamber, we used 1 nM EcoRV in all experiments (see *Materials and Methods*).

Rate Acceleration on Coiled DNA. Specific association rates k_{on} were computed from 385 individual cleavage reactions (see *Materials and Methods*). Variation of the DNA configuration includes three regimes (see Fig. 1*C*): (*i*) extended DNA, where jumping to different DNA segments cannot take place (≈1 pN tension, ≈85% extended); (*ii*) a DNA configuration that is close to a relaxed coil (fractional extension a between 0.2 and 0.3; and (*iii*) smaller fractional extensions, where the beads interfere with the coil and the DNA is slightly squeezed out of the narrow gap. Fig. 4 shows the association rates acquired for different DNA conformations. Strikingly, at 100 mM NaCl the specific association rate on DNA held in an extended configuration is almost twice as slow as on coiled DNA. We define R as the ratio between the maximal association rate and the rate found on stretched DNA. The fastest association is measured at $a = 0.24$ ($R = 1.7 \pm 0.3$). At smaller extensions, a decrease in the rate occurs. Why would the search rate acceleration peak at a fractional extension of 0.24? A relaxed pCco5 DNA molecule (6,538 bp) with free ends would form a coil with a mean square end-to-end distance $\langle R_e^2 \rangle \approx 2Ll_p \approx (0.49\ \mu m)^2$ (29), corresponding to $a = 0.22$. The maximal association rate is thus found at the extension where DNA is closest to its free random configuration. We attribute the rate difference with stretched DNA to the disappearance of intersegmental jumping in stretched DNA (Fig. 1 *A* and *B*). At $a \leq 0.2$, the presence of the two large beads causes a deformation of the DNA coil. In addition to possible obstruction of enzyme access routes, on average the local density of DNA segments around the specific site l_{DNA} will be lower than for the relaxed coil, resulting in the observed decrease in association rate. The second-order association rate constants deduced from the single-molecule cleavage events, $1.8 \pm 0.2 \times 10^8\ M^{-1}{\cdot}s^{-1}$ in the coiled configuration is in close agreement with values found earlier in bulk experiments in similar buffers: $1.2–2.2 \times 10^8\ M^{-1}{\cdot}s^{-1}$ (30–33).

Salt Dependence of Association Rate. Nonspecific protein–DNA interactions are largely of electrostatic nature and therefore depend on salt concentration (34). Changes in buffer conditions could thus induce a shift in the relative contributions of 1D and

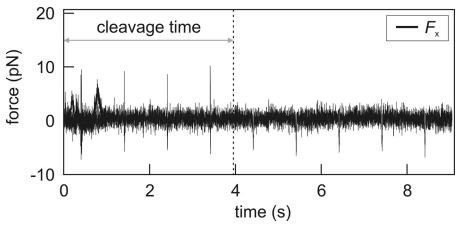

Fig. 2. Typical data trace of a cleavage event. Displayed is the force on the DNA in the direction along the stretched molecule. Every second, the DNA is rapidly stretched to ≈5–10 pN, resulting in sharp positive force spikes (negative spikes are caused by the fast movement of the beads and do not represent a real force on the DNA). Disappearance of these spikes implies that the DNA molecule has been cleaved in the preceding second. The best estimate for this event is exactly halfway between the last spike and the next stretching attempt. We thus define the reaction time as the time between transportation of the DNA construct into the enzyme-containing flow channel ($t = 0$ in the graph) and last upward spike plus 0.5 s. The statistical error that is introduced in the measured cleavage time (≈0.5 s) averages out for the large number of data points.

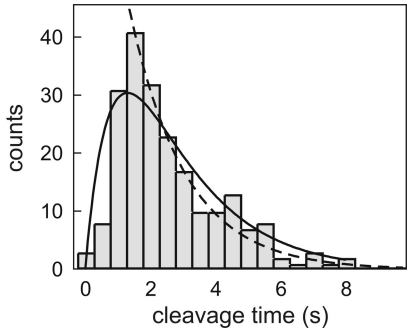

Fig. 3. Determination of DNA hydrolysis rate, obtained with 500 nM EcoRV in reaction buffer with 100 mM NaCl. Because in the optical tweezers experiments only the cleavage of the second strand is observed, the distribution of cleavage times shows a lag phase. The single exponential fit (dashed line) gives a strand cleavage rate k_1 of $0.60 \pm 0.03\ s^{-1}$ for the second strand. Because of degeneracy, cleavage of the first strand should in principle be twice as fast. As a result, the rate of hydrolysis for both DNA strands is $0.40 \pm 0.03\ s^{-1}$. The average time required for DNA cleavage is the inverse, 2.5 ± 0.2 s. The full distribution can also directly be fitted with such a two-step process ($k_1[\exp(-k_1 t) - \exp(-2k_1 t)]$). Doing so (solid line) yields a strand cleavage rate k_1 of $0.54 \pm 0.03\ s^{-1}$, comparable to the rate found above.

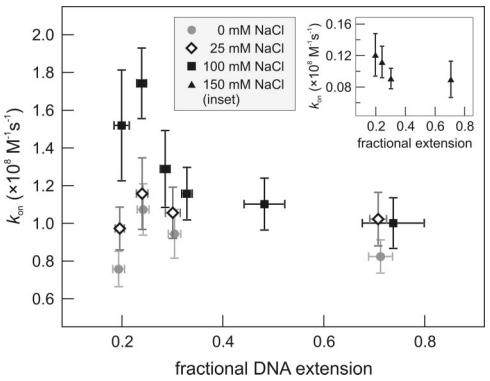

Fig. 4. EcoRV association rates to the single recognition site on linear DNA molecules as a function of DNA extension. In 100 mM NaCl the association rate is found to be maximal around a fractional extension $a \approx 0.22$, and decreases rapidly for increasing extensions, reducing almost a factor of two as the DNA is stretched. This effect is attributed to loss of intersegmental jumping in the search process of EcoRV. At low fractional extensions the DNA coil is deformed by the beads, resulting in a lowered local density of DNA segments around the recognition site. At lower salt conditions (0 and 25 mM) this effect disappears. (*Inset*) Association rates in 150 mM NaCl are ≈10-fold lower for all DNA extensions. Each data point consists of a minimum of 30 measurements.

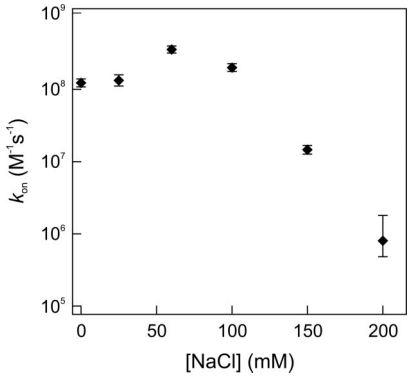

Fig. 5. EcoRV association rates measured on coiled DNA as a function of salt concentration, showing an optimum at ≈60 mM NaCl. (At this particular concentration, DNA hydrolysis becomes the rate-limiting step.) For NaCl concentrations >100 mM, the association rate of EcoRV to the specific site decreases exponentially.

3D pathways in the search process. To examine this effect, we repeated the cleavage measurements on relaxed and extended DNA in buffers with different NaCl concentrations (Fig. 4). At 0 and 25 mM NaCl we observed almost invariable association rates for all DNA extensions, indicating a lowered probability of protein jumping. We found an optimal salt concentration for target finding at 60 mM, consistent with previous biochemical assays (18, 19). Apparently, at this salt concentration the effective sliding length l_{sl}^{eff} (the average length of correlated motion along the contour of the DNA, including both hopping and sliding) is maximal. However, we could not probe the difference between the stretched and coiled DNA configuration at 60 mM NaCl. At that concentration the EcoRV association rate approaches the rate of phosphodiester hydrolysis (0.4 s^{-1}), causing the reaction to be rate-limited by this process instead of by diffusion. Using a lower EcoRV concentration could diminish this problem, but as mentioned before we detected fluctuations in the actual amount of enzymes present in the flow chamber if we decreased the EcoRV concentration <1 nM. In reaction buffers containing 150 and 200 mM NaCl, target site location rates were dramatically lowered for all DNA configurations, probably attributable to the reduced affinity of EcoRV for both specific and nonspecific DNA in these buffers (35) (Figs. 4 *Inset* and 5). Here, the sliding length became so small that the enzyme effectively performed a 3D random walk and facilitation by nonspecific binding was absent.

Theoretical Modeling of Intersegmental Jumping. To quantitatively explain the enzyme's acceleration of target site association, we consider EcoRV's search for the specific cleavage site as a combination of (*i*) sliding diffusion along the DNA with diffusivity D_{1d}, until dissociation to the bulk (with rate k_{off}^{ns}) and (*ii*) 3D diffusion with diffusivity D_{3d} where an enzyme eventually (re)binds nonspecifically to a DNA segment (with rate per length k_{on}^{ns}). Eventually, the target is found with rate k_{on}.

Below we describe two limiting cases. If 3D diffusion were much faster than nonspecific binding, i.e., $D_{3d} \gg k_{on}^{ns}$ (k_{on}^{ns} has units of inverse concentration per length per time, i.e., length squared per time like D_{3d}), an enzyme would perform a long diffusive volume excursion in the bulk before rebinding to the DNA, losing its correlation to the previous dissociation site. The search rate would then be $k_{on} = 2\, k_{on}^{ns} l_{sl}$, with sliding length $l_{sl} = (D_{1d}/\, k_{off}^{ns})^{1/2}$ (11): typically only proteins binding nonspecifically within a distance l_{sl} from the target will actually find it. In this case the global conformation of the DNA would not influence the search dynamics, in contrast to what we observed for EcoRV.

Conversely, if $D_{3d} \ll k_{on}^{ns}$ an enzyme just dissociated from the DNA is likely to rebind immediately. k_{on} will then be smaller than $2\, k_{on}^{ns} l_{sl}$, as the enzyme will often slide along previously visited DNA segments, an inefficient oversampling (Fig. 1*A*). The effective sliding length $l_{sl}^{eff} = [k_{on}^{ns}/(2\pi D_{3d})]^{1/2} l_{sl}$ (36) is a measure of the distance, including intrasegmental (microscopic) hops, that the protein explores before effectively leaving a DNA segment. Experiments suggest that l_{sl}^{eff} for EcoRV can be as large as hundreds of base pairs (18, 20). Analysis by Zhou *et al.* (13) of these experimental data gives the maximal value of the ratio $K'_{ns} = D_{1d}\, k_{on}^{ns}/(D_{3d}\, k_{off}^{ns})$ as 5.2×10^3 $M^{-1}{\cdot}bp^{-1}$. In terms of effective sliding this corresponds to $l_{sl}^{eff} = \sqrt{K'_{ns}/(2\pi)} = 193$ bp (using 1 bp = 0.34 nm). However, for such a l_{sl}^{eff} one would expect a search rate $\approx D_{3d} l_{sl}^{eff}$ of order 10^{10} $M^{-1}{\cdot}s^{-1}$, much faster than k_{on} $\approx 10^8$ $M^{-1}{\cdot}s^{-1}$ found experimentally. More precisely, using $l_{sl}^{eff} =$ 193 bp one can use the expression for k_{on} on infinitely long stretched DNA as discussed in ref. 36 to arrive at an expected k_{on} $\approx 2 \times 10^{10}$ $M^{-1}{\cdot}s^{-1}$ (a result that is essentially independent of the detailed choice of D_{1d}, k_{off}^{ns}, etc.). To explain the *a priori* unexpectedly low experimental rate we follow an observation by Erskine *et al.* (30): based on x-ray crystallography data, EcoRV may switch between an open state allowing for DNA binding, and a closed one that does not. The actual rate constant becomes $k_{on} = x_{act} k_{on}^{act}$, x_{act} being the fraction of open (and therefore active) EcoRV and k_{on}^{act} its association rate constant. Assuming that $k_{on} \approx 1.5 \cdot 10^8$ $M^{-1}{\cdot}s^{-1}$ for stretched DNA when $l_{sl}^{eff} = 193$ bp and $k_{on}^{act} \approx 2 \times 10^{10}$ $M^{-1}{\cdot}s^{-1}$ this gives $x_{act} \approx 0.75\%$. Physiologically, the advantage of this open/closed isomerization could be to provide the cell with a reservoir of EcoRV uniformly distributed in the cytoplasm, instead of being bound nonspecifically to the cell's own DNA. Foreign DNA entering the cell would then immediately be surrounded by a higher concentration of EcoRV that, after switching to the open state, could readily attack the foreign DNA.

So why does coiled DNA enable faster target search than stretched DNA? An enzyme that would otherwise rebind quickly to the segment it just visited can instead be captured by another segment, that is nearby (in 3D space) because of DNA looping (Fig. 1*B*). This conversion from an intrasegmental hop to an intersegmental jump reduces oversampling, because in chemical distance along the DNA the dissociation and rebinding points are remote. Given an escape time from a segment of typical

Table 1. Fitting parameters and the corresponding theoretical value of *R* (see *SI Appendix*) compared with the measurements

[NaCl], mM	$k_{on}^{straight}$, $(M{\cdot}s)^{-1}$	l_{sl}^{eff}, bp	$1/\sqrt{l_{DNA}}$, bp	R_{theory}	$R_{measured}$
0	0.8×10^8	97	518	1.11	1.3
25	1.0×10^8	123	485	1.15	1.1
100	1.0×10^8	122	120	1.63	1.7
150	0.09×10^8	9.1	80	1.10	1.3

The measured on rates for extended DNA, $k_{on}^{straight}$, are used as input for the theory to obtain the values of l_{sl}^{eff} assuming that the estimate $x_{act} = 0.75\%$ holds for all [NaCl].

order of 1 s (30), and with the estimate of 2 ms for the polymer configuration relaxation time (see *Materials and Methods*), one sees that the polymer configuration will change in between intersegmental jumps, such that successive intersegmental jumps are likely to occur at a point that also in 3D space is remote from the original segment. These considerations are quantified in *SI Appendix*, in which the work of Berg and Ehrenberg (36), where the DNA was treated as a straight cylinder, is generalized to the coiled configuration by including also foreign segments around the target site as randomly placed straight cylinders. This procedure allows us to estimate the probability of intrasegmental hops of different lengths being converted into intersegmental jumps, and how this affects the search rate k_{on}. In Table 1 we list values for the relative acceleration R caused by coiling resulting from this theoretical modeling. The fitting parameters were chosen such that consistency is achieved simultaneously with both DNA extension and [NaCl] variation and with previously published values. The value of R is found to rise above unity when l_{sl}^{eff} is comparable with or larger than the typical distance $l_{DNA}^{-1/2}$ between DNA segments, where l_{DNA} is the average density (length per volume) of foreign DNA segments around the specific target site. We interpret the high value of R at 100 mM NaCl in terms of an increased l_{DNA} because of a mutual attraction of DNA segments at these salt conditions. Such attraction was predicted by Lee *et al.* (37) from molecular dynamics simulations. Moreover, Qui *et al.* (38) experimentally demonstrated that such attraction exists between 25-bp DNA pieces above Mg^{2+} concentrations of 16 and 10 mM in cases with, respectively, no monovalent salt and 20 mM NaCl present. In our experiments with 5 mM Mg^{2+} we expected the onset of DNA attraction to occur between 20 and 100 mM NaCl. Table 1 reflects this expected increase of DNA density.

Previously, a 3-fold preference of cleaving supercoiled plasmids over relaxed plasmids was observed (17), in qualitative agreement with our results: whereas the density of DNA segments in supercoiled DNA is larger than in a relaxed coil, the density of DNA in the coiled state is larger than when it is held straight. Hence, the amount of reassociations to nearby DNA segments decreases from many to a few in the supercoiling experiment and from a few to zero in our experiment. Combining both studies thus demonstrates already a 6-fold enhancement of the searching rate of restriction enzymes caused by intrasegmental jumping. Considering that in the cell the density of DNA is even higher (because of crowding, condensing agents, and DNA-organizing proteins), we can conclude that *in vivo* the jumping pathway is an essential tool for efficiently targeting specific sites on DNA.

Materials and Methods

Experiments. EcoRV was recovered from ammonium sulfate precipitates as described (26). For the DNA cleavage experiments pCco5 plasmid (6.5 kbp in length) was linearized by SpeI digestion (25). The linear DNA contains a single recognition site located almost in the middle. The degree of DNA coiling was controlled by changing the distance between the two attached beads.

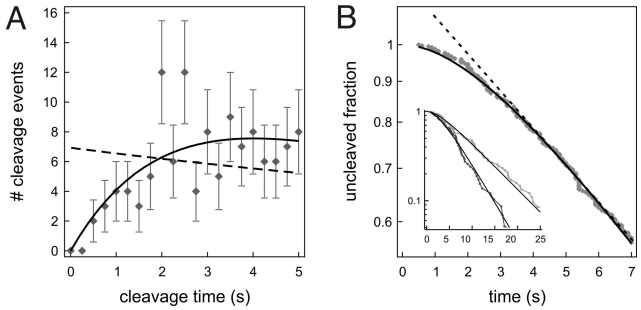

Fig. 6. The effect of hydrolysis on the measured cleavage rates, performed on data taken in 100 mM NaCl. For increased statistics data from all DNA conformations are combined here. (*A*) The first part of the distribution of cleavage times (0.25-s time bins) shows a lag phase caused by the presence of DNA hydrolysis as a second step in the reaction. The dashed line is the single-exponential fit (to the full distribution), and the solid curve is the fit for a two-step process. The hydrolysis rate (for the cleavage of both DNA strands) obtained by the fit is $0.4 \pm 0.1\ s^{-1}$, in accordance with the direct measurements of this parameter (Fig. 3). (*B*) Probability distribution of cleavage time, constructed from the same data as in *A*. Also in this representation a two-step process (solid line) describes the data more accurately than a single exponential (dashed line), signifying the presence of DNA hydrolysis (again with a rate of $0.4 \pm 0.1\ s^{-1}$). (*Inset*) Probability distributions for data subsets with the smallest (black) and largest (gray) fractional extensions. Although this method may provide an ''easy way out'' for fitting both hydrolysis and association rate, the uncertainties of the fits are ill-defined, as the individual data points in this cumulative representation are not independent.

A detailed description of the experimental setup is given in ref. 26. Because of nonmixing laminar buffer flow (39), assembled DNA constructs can be transported into a channel containing 1 nM EcoRV with an estimated timing error of 0.5 s. Before each experiment session a 10 mM Tris·HCl buffer (pH 7.5) containing 1 mg/ml BSA was flowed through the chamber for ≈30 min to coat the walls of the chamber and tubing to prevent sticking of EcoRV enzymes. The enzyme reaction buffer contained 10 mM Tris·HCl (pH 7.5), 5 mM $MgCl_2$, 1 mM DTT, 100 μg/ml BSA, and a variable NaCl concentration. During the cleavage time measurements the buffer flow was stopped to allow undisturbed spatial fluctuations in the DNA molecule held at a certain extension. This configuration was only transiently abandoned to a stretched conformation once per second to check for DNA cleavage. The stretching was done by rapid translation of one of the optical traps, controlled by an acousto-optic deflector (Movie S1). Before the recording of each data point, the flow was switched on for a minimum of 2 min (at ≈100 μm/s) to re-equilibrate the enzyme concentration and ensure sharp borders between different flow channels. The various fractional extensions explored were alternated sequentially during experiments to rule out possible influence of small variations in enzyme and/or salt concentrations on longer timescales.

Determination of Specific Association Rates. Specific association rates at the different DNA conformations were calculated from the average measured time required for cleavage on >30 DNA molecules at each DNA conformation for each NaCl concentration. For a one-step Poissonian process, the average of measured cleavage times equals the time constant of an exponential fit to the time-binned histogram. However, the cleavage of an individual DNA molecule in our experiments is effectively a multistep process, comprising both association to the specific site and DNA hydrolysis of both strands. At the used EcoRV concentration of 1 nM the association step is mostly rate-limiting (except at 60 mM NaCl). Yet, a histogram computed from the total of 385 events at 100 mM NaCl (shown in Fig. 6) still shows a lag phase for small cleavage times (with rate $0.4\ s^{-1}$), owing to DNA hydrolysis (both strands), followed by an exponential drop-off. Consequently, by computing the rate simply from the averages of measured cleavage times, one would underestimate the actual association rate. We therefore corrected for DNA hydrolysis by subtracting the average hydrolysis time (2.5 s; see Fig. 3) from the statistical average of the measured cleavage time. The association rate is the inverse of this number (see *SI Appendix* for details).

Relaxation Time of DNA Fluctuations. The DNA between the beads undergoes constant thermal fluctuations. The transient stretching cycles could in principle lead to an enhanced mixing of DNA conformational states if the duration

BIOPHYSICS

of the stretch is shorter than the relaxation time τ_R of the coiled polymer. The latter can be calculated by using the Rouse model (40, 41):

$$\tau_R = \frac{2l_P L^2 \eta}{3\pi \ln(L/d) k_B T}.$$

With a persistence length $l_p = 50$ nm, DNA diameter $d = 2$ nm, contour length $L = 2.2$ μm, η as the viscosity of the buffer ($\approx 10^{-3}$ Pa·s), and k_BT as the thermal energy, we obtain $\tau_R \approx 2$ ms. Compared with the stretching duration (<20 ms) this is fast enough to exclude any enhanced mixing.

EcoRV Concentration. We determined the average hydrolysis time for the cleavage of both strands to be 2.5 s (Fig. 3). To make association rate-limiting, a minimum cleavage time of $\approx$10 s or more is required. With a specific association rate on plasmids of $\approx 10^8$ $M^{-1}{\cdot}s^{-1}$ (30), this requires an enzyme concentration $\leq$1 nM. Because at low [EcoRV] the specific association rate is proportional to the enzyme concentration, it is crucial that the number of enzymes in the flow chamber is constant in all measurements. To test which protein concentration still yields reliable results we performed cleaving experiments with progressively lower proteins concentrations. For each concentration we determined the average cleaving times for independent sets of trial experiments (i.e., a new protein dilution used in a cleaned or new flow chamber). These tests showed that for EcoRV concentrations <0.7 nM the average cleavage times differed by up to $\approx$50% between data sets, presumably caused by proteins sticking to and detaching from the walls of the chamber and tubing. At concentrations $\geq$1 nM such effects were never observed. Therefore, 1 nM EcoRV was used in the experiments.

ACKNOWLEDGMENTS. We thank Dave Hiller, John Perona, Tobias Ambjörnsson, Alexander Grosberg, and Roland Winkler for helpful discussions. This work was supported by a Fundamenteel Onderzoek der Materie Projectruimte Grant, a Netherlands Organization for Scientific Research-Vernieuwings-Impuls grant (to G.J.L.W.), and the Villum Kann Rasmussen Foundation (M.A.L.).

1. Browning DF, Busby SJ (2004) The regulation of bacterial transcription initiation. *Nat Rev Microbiol* 2:57–65.
2. Garvie CW, Wolberger C (2001) Recognition of specific DNA sequences. *Mol Cell* 8:937–946.
3. Riggs AD, Bourgeois S, Cohn M (1970) The lac repressor-operator interaction. 3. Kinetic studies. *J Mol Biol* 53:401–417.
4. Berg OG, Winter RB, von Hippel PH (1981) Diffusion-driven mechanisms of protein translocation on nucleic acids. 1. Models and theory. *Biochemistry* 20:6929–6948.
5. Winter RB, Berg OG, von Hippel PH (1981) Diffusion-driven mechanisms of protein translocation on nucleic acids. 3. The *Escherichia coli* lac repressor–operator interaction: Kinetic measurements and conclusions. *Biochemistry* 20:6961–6977.
6. Dhavan GM, Crothers DM, Chance MR, Brenowitz M (2002) Concerted binding and bending of DNA by *Escherichia coli* integration host factor. *J Mol Biol* 315:1027–1037.
7. Gowers DM, Wilson GG, Halford SE (2005) Measurement of the contributions of 1D and 3D pathways to the translocation of a protein along DNA. *Proc Natl Acad Sci USA* 102:15883–15888.
8. Halford SE, Marko JF (2004) How do site-specific DNA-binding proteins find their targets? *Nucleic Acids Res* 32:3040–3052.
9. Coppey M, Benichou O, Voituriez R, Moreau M (2004) Kinetics of target site localization of a protein on DNA: A stochastic approach. *Biophys J* 87:1640–1649.
10. Hu T, Grosberg AY, Shklovskii BI (2006) How proteins search for their specific sites on DNA: The role of DNA conformation. *Biophys J* 90:2731–2744.
11. Lomholt MA, Ambjornsson T, Metzler R (2005) Optimal target search on a fast-folding polymer chain with volume exchange. *Phys Rev Lett* 95:260603.
12. Slutsky M, Mirny LA (2004) Kinetics of protein-DNA interaction: Facilitated target location in sequence-dependent potential. *Biophys J* 87:4021–4035.
13. Zhou HX (2005) A model for the mediation of processivity of DNA-targeting proteins by nonspecific binding: Dependence on DNA length and presence of obstacles. *Biophys J* 88:1608–1615.
14. Wunderlich Z, Mirny LA (2008) Spatial effects on the speed and reliability of protein-DNA search. *Nucleic Acids Res* 36:3570–3578.
15. Lomholt MA, Koren T, Metzler R, Klafter J (2008) Lévy strategies in intermittent search processes are advantageous. *Proc Natl Acad Sci USA* 105:11055–11059.
16. von Hippel PH, Berg OG (1989) Facilitated target location in biological systems. *J Biol Chem* 264:675–678.
17. Gowers DM, Halford SE (2003) Protein motion from nonspecific to specific DNA by three-dimensional routes aided by supercoiling. *EMBO J* 22:1410–1418.
18. Jeltsch A, Pingoud A (1998) Kinetic characterization of linear diffusion of the restriction endonuclease EcoRV on DNA. *Biochemistry* 37:2160–2169.
19. Jeltsch A, Wenz C, Stahl F, Pingoud A (1996) Linear diffusion of the restriction endonuclease EcoRV on DNA is essential for the *in vivo* function of the enzyme. *EMBO J* 15:5104–5111.
20. Stanford NP, Szczelkun MD, Marko JF, Halford SE (2000) One- and three-dimensional pathways for proteins to reach specific DNA sites. *EMBO J* 19:6546–6557.
21. Wang YM, Austin RH, Cox EC (2006) Single-molecule measurements of repressor protein 1D diffusion on DNA. *Phys Rev Lett* 97:048302.
22. Sokolov IM, Metzler R, Pant K, Williams MC (2005) Target search of N sliding proteins on a DNA. *Biophys J* 89:895–902.
23. Blainey PC, van Oijen AM, Banerjee A, Verdine GL, Xie XS (2006) A base-excision DNA-repair protein finds intrahelical lesion bases by fast sliding in contact with DNA. *Proc Natl Acad Sci USA* 103:5752–5757.
24. Kim JH, Larson RG (2007) Single-molecule analysis of 1D diffusion and transcription elongation of T7 RNA polymerase along individual stretched DNA molecules. *Nucleic Acids Res* 35:3848–3858.
25. van den Broek B, Noom MC, Wuite GJL (2005) DNA-tension dependence of restriction enzyme activity reveals mechanochemical properties of the reaction pathway. *Nucleic Acids Res* 33:2676–2684.
26. Noom MC, van den Broek B, van Mameren J, Wuite GJ (2007) Visualizing single DNA-bound proteins using DNA as a scanning probe. *Nat Methods* 4:1031–1036.
27. Halford SE, Goodall AJ (1988) Modes of DNA cleavage by the EcoRV restriction endonuclease. *Biochemistry* 27:1771–1777.
28. Taylor JD, Halford SE (1989) Discrimination between DNA sequences by the EcoRV restriction endonuclease. *Biochemistry* 28:6198–6207.
29. Grosberg AY, Khokhlov AR (1994) *Statistical Physics of Macromolecules* (AIP Press, New York).
30. Erskine SG, Baldwin GS, Halford SE (1997) Rapid-reaction analysis of plasmid DNA cleavage by the EcoRV restriction endonuclease. *Biochemistry* 36:7567–7576.
31. Erskine SG, Halford SE (1998) Reactions of the EcoRV restriction endonuclease with fluorescent oligodeoxynucleotides: Identical equilibrium constants for binding to specific and nonspecific DNA. *J Mol Biol* 275:759–772.
32. Hiller DA, *et al.* (2003) Simultaneous DNA binding and bending by EcoRV endonuclease observed by real-time fluorescence. *Biochemistry* 42:14375–14385.
33. Hiller DA, Rodriguez AM, Perona JJ (2005) Noncognate enzyme–DNA complex: Structural and kinetic analysis of EcoRV endonuclease bound to the EcoRI recognition site GAATTC. *J Mol Biol* 354:121–136.
34. Lohman TM (1986) Kinetics of protein–nucleic acid interactions: Use of salt effects to probe mechanisms of interaction. *CRC Crit Rev Biochem* 19:191–245.
35. Engler LE, Welch KK, Jen-Jacobson L (1997) Specific binding by EcoRV endonuclease to its DNA recognition site GATATC. *J Mol Biol* 269:82–101.
36. Berg OG, Ehrenberg M (1982) Association kinetics with coupled three- and one-dimensional diffusion. Chain-length dependence of the association rate of specific DNA sites. *Biophys Chem* 15:41–51.
37. Lee KC, Borukhov I, Gelbart WM, Liu AJ, Stevens MJ (2004) Effect of mono- and multivalent salts on angle-dependent attractions between charged rods. *Phys Rev Lett* 93:128101.
38. Qiu X, *et al.* (2006) Measuring inter-DNA potentials in solution. *Phys Rev Lett* 96:138101.
39. Brewer LR, Corzett M, Balhorn R (1999) Protamine-induced condensation and decondensation of the same DNA molecule. *Science* 286:120–123.
40. Doi M, Edwards, SF (1986) *The Theory of Polymer Dynamics* (Oxford Science, Oxford).
41. Li L, Hu H, Larson RG (2004) DNA molecular configurations in flows near adsorbing and nonadsorbing surfaces. *Rheol Acta* 44:38–46.